Photovoltaic performance of pristine and arsenic doped hybrid perovskite

N. Sharma[a], P. Tiwari[b], S. Choudhary[c], M. Mittal[a], A. Saini[a], P. Singh[d], D. Saraswat[b], A. Kumari[e], A. S. Verma[f,g,*]
[a]*Department of Physics, Dhanauri P.G. College, Dhanauri, Haridwar, Uttarakhand, 247667, India*
[b]*Department of Physical Sciences, Banasthali Vidyapith, Rajasthan, 304022, India*
[c]*Department of Physics, Constituent Government Degree College, Richha Baheri, Bareilly, 243201, India*
[d]*Department of Electronics and Communication Engineering, KIET Group of Institutions, Ghaziabad, 201206, India*
[e]*Department of Physics, S. V. College, Raja Mahendra Pratap Singh State University, Aligarh, 202140, India*
[f]*Division of Research and Innovation, School of Applied and Life Sciences, Uttaranchal University, Dehradun, 248007, India*
[g]*University Centre for Research & Development, Department of Physics, Chandigarh University, Mohali, Punjab, 140413, India*

Under the scope of all-solid-state perovskite solar cells, the important role of methyl-ammonium lead halide film lies in facilitating the formation of a photo-generated electron-rich film, which directly affects the overall photovoltaic performance. This study introduces a novel chemical strategy aimed at increasing the quality of perovskite film through minimal arsenic doping. The result of the inclusion of arsenic is characterized by high crystalline grains in the attainment of a homogeneous, uniform and ancient perovskite film. The analysis of the UV-Visible spectra indicates that the perovskite film, which is produced under sequential conditions, displays light extraction of electrons for light absorption, more effective electron transport, and adjacent electron transport layer. Different morphology obtained through customized perovskite conditions contribute to a better short-circuits current, which improves overall cell performance. Arsenic-doped perovskite-based solar cells demonstrate a 1.55% increase in power conversion efficiency compared to their non-decorated counterparts, exhibiting 0.20% efficiency. The outcomes not only offer a straightforward method for enhancing perovskite films but also introduce an innovative perspective on constructing high-performance perovskite solar cells using minimal amounts of arsenic, thereby minimizing toxicity in the fabricated solar cells.

(Received April 26, 2024; Accepted July 18, 2024)

Keywords: Hybrid perovskite, UV-Visible spectra, FE-SEM, I-V curve

1. Introduction

The global energy crises and increased energy consumption is major issue in environmental and economic aspects expected to rise rapidly in the coming years. Although fossil fuels are the leading source of energy and presently dominate the energy market, they are depleting and tend to cause negative environmental effect [1–4]. The solution to these problems may lie in the developing the environmentally safe, sustainable and affordable alternate energy sources. In this context, photovoltaic technology especially based on organic materials has shown the huge potential for the development of affordable and sustainable electricity sources for the future [5–9]. Despite providing the unique advantages, typically Organic Solar Cells (OSCs) suffer from the inadequate efficiency and durability issues. With the advent of the Bulk Heterojunction (BHJ) concept in OSCs, the efficiency has been boosted to over 10 %. However, insufficiency in photon harvesting of the active

* Corresponding author: ajay_phy@rediffmail.com
https://doi.org/10.15251/JOR.2024.204.505

layer due to the narrow absorption window (~100 nm) of organic semiconductors hindered further enhancement in the performance of single-junction OSCs [10–13].

In recent years, the perovskite solar cell has garnered significant attention as a promising solar power technology, owing to its impressive attributes such as high Power Conversion Efficiency (PCE), cost-effectiveness in production, and simple fabrication processes. The pioneering work by Kojima et al. [14] have marked the initiation of perovskite solar cell research, demonstrating a PCE of 3.8%. Afterwards, Lee et al. [15] have pioneered the use of mixed halide perovskite, especially $CH_3NH_3PbI_2Cl$, resulting in a prominent enhancement of PCE to 10.9%. This initial development stimulated prevalent rate of interest leading various study teams to explore the research study of perovskite solar batteries. With continual initiatives, considerable strides have been made, with the present PCE standing at an excellent 25.7%. The fast renovation in PCE highlights the capacity of perovskite-structured products in the developing area of Photovoltaics [16].

The use of organic-inorganic lead halide perovskite solar batteries has become a very appealing modern technology for progressing Photovoltaics mainly owing to its exceptional PCE plus the ease of manufacture via a very easy option procedure. Nevertheless, the poisoning related to lead in perovskite has triggered an expedition right into alternative, safe alkaline planet steel cations as sensible substitutes [17-19]. Perovskite solar batteries stand for an ingenious photovoltaic innovation that has displayed exceptional improvements in effectiveness, paired with the ease of standard service procedures. A vital emphasis in the search for high-performance Perovskite solar batteries hinges on the growth of lead-free or lead-reduced Perovskite materials [20]. This imperative arises from the environmental and health concerns associated with lead-based materials. Within the category of alkaline earth metals, strontium (Sr^{2+}) and barium (Ba^{2+}) emerge as promising candidates for replacing lead (Pb^{2+}) in perovskite films. This substitution is facilitated by the favourable fit of Goldschmidt's tolerance factor, ensuring the structural integrity of the perovskite lattice [21–23].

Herein, we have done the doping of Arsenic in pristine perovskites and have characterized the sample with different characterization and have studied the structural, optical and electrical properties.

1.1 Material

Methyl-ammonium Iodide (MAI (CH_3NH_3I)) and Lead Iodide (PbI_2) have been procured from Sigma Aldrich, while anhydrous N, N-dimethyl-formamide (DMF) has been obtained from Merck and employed as a solvent for the synthesis of CH_3NH_3I and Lead chloride ($PbCl_2$) compounds. All materials have been utilized in their as-received state without undergoing additional purification, ensuring the integrity and reproducibility of the experimental procedures.

1.2. Synthesis of CH_3NH_3I

MAI and CH_3NH_3I are synthesized through the reaction between methylamine (24 ml, 33 wt% in pure ethanol) and Hydroiodic Acid (10 ml, 57 wt% in water) at 0°C in an ice bath, with continuous stirring over 2 hours. Subsequently, the resulting white crystalline solid was obtained by evaporating the mixture at 50°C for 1 hour. The synthesized material undertook a detailed cleaning procedure with diethyl ether, repeated three times. Eventually the depolluted white powder (MAI and CH_3NH_3I) is obtained as well as based on overnight drying out in a vacuum cleaner stove at 60°C. This entire synthesis process is dynamic for generating high-grade MAI, validating its purity and suitability for additional research applications.

1.3. Synthesis of Perovskite precursor

In 2 millilitres (ml) of dimethyl-formamide (DMF), MAI and PbI_2 must disintegrate at a 3:1 molar ratio for it to produce $CH_3NH_3PbI_3$. To ensure homogeneity, the preliminary mixture was continuously stirred throughout the night to generate the homogenous predecessor solution. This procedure is crucial to assembly high-quality $CH_3NH_3PbI_3$ for potential applications in research and technology.

1.4. Fabrication of device

The arsenic-doped perovskite was made using a new procedure that involved dissolving PbI2 (1.2 M) and MAI (1.11 M) in anhydrous N, N′-DMF mixture. Next, the perovskite solutions are spin-coated for 15 seconds at 3000 rpm in a single process. The arsenic iodide solution is applied to the perovskite layer after 30 seconds. After that, the films are annealed for 15 minutes at 100°C. Notably, all the film preparation steps are meticulously executed within a nitrogen-filled glove box to maintain controlled environmental conditions. To enhance the properties of the perovskite film, a layer of aluminium (Al) was deposited using the thermal evaporation technique.

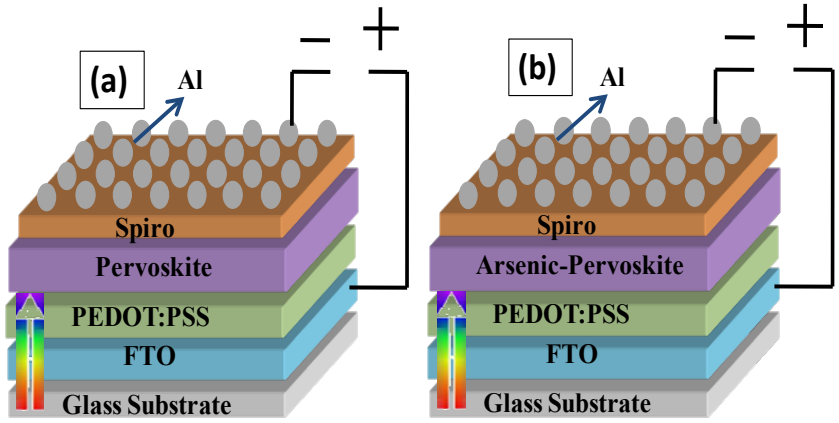

Fig. 1. Absorption spectra (a) D1-Pristine Perovskite, (b) D2-Arsenic doped perovskite.

Two devices, designated as D1 and D2, have been fabricated using the aforementioned methodology as presented in Figure 1 (a-b). Figure 1(a) represents the absorption spectra of D1-Pristine Perovskite, and Figure 1(b) represents D2-Arsenic doped perovskite.

- **D1 : FTO / PEDOT:PSS/ Perovskite / Spiro / Al**
- **D2 : FTO/ PEDOT:PSS / As doped perovskite / Spiro / Al**

2. Result and discussion

Figure 2 presents the absorbance spectra of arsenic-doped perovskite and pure perovskite, revealing notable modifications in the UV- visible spectra.

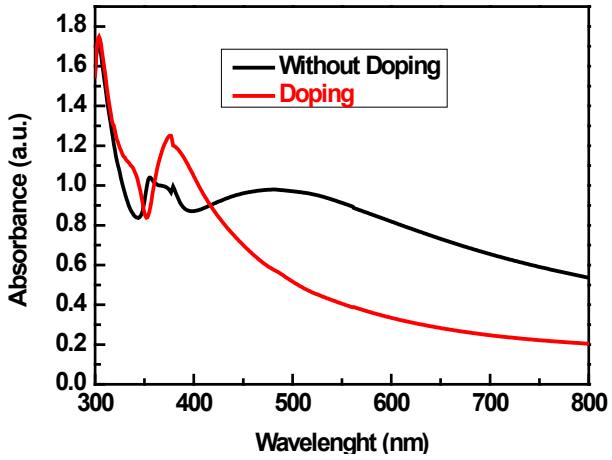

Fig. 2. Absorption spectra of Perovskite and Arsenic doped perovskite.

A distinct peak of $MAPbI_3$ is observable around 400 nm. The introduction of Arsenic doping significantly influences the absorbance spectra, enhancing the light absorption of $MAPbI_3$ from 350 nm to approximately 800 nm.

This enhancement suggests that Arsenic plays a crucial role in extending the range of light absorption in $MAPbI_3$. An analysis of the UV-visible spectra of the initial PbI_2 films indicates an absorption onset at 515 nm (2.4 eV) with an excitonic peak at 495 nm. Further absorption, escalating towards the UV region, is also observed. Wavelengths beyond 515 nm reveal interference patterns, indicating a smooth and uniformly thick spin-coated PbI_2 layer. Notably, a peak emerges between 500 nm and 700 nm, and its intensity increases with higher concentrations of $MAPbI_3$ [24].

To gain deeper insights into the morphological changes during the conversion from pristine Perovskite to As-doped Perovskite, we employed Field Emission Scanning Electron Microscopy (FESEM), as illustrated in Figure 3. In both cases, significant morphological transformations are evident. In Figure 3(a) we can the traps in the morphology of pristine Perovskite which is not a good symbol for device fabrication. Smooth and same grain size morphology has been observed in Figure 3(b). From morphology study we can say that smooth surface based device can provide path for charge carrier to reach their respective electrodes [25].

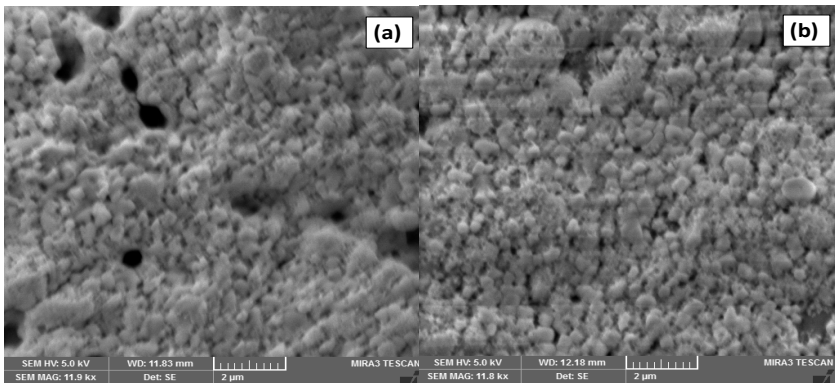

Fig. 3. FESEM images of (a) Pristine Perovskite, (b) Doping of Arsenic with Perovskite.

In the perovskite film, isolated perovskite crystals appear on the surface within the PbI_2 matrix. Conversely, in the Arsenic-doped films, the small elongated grains undergo a transformation into larger, more rectangular grains. This observation emphasizes the impact of Arsenic doping on the evolution of the thin film's surface morphology during the conversion process.

Figure 4 illustrates the Energy Dispersive X-ray Spectrometry (EDS) images of perovskite samples, comparing un-doped and Arsenic-doped variations. Employing FESEM with EDS, a widely utilized elemental microanalysis technique in various scientific disciplines, we conducted a comprehensive examination.

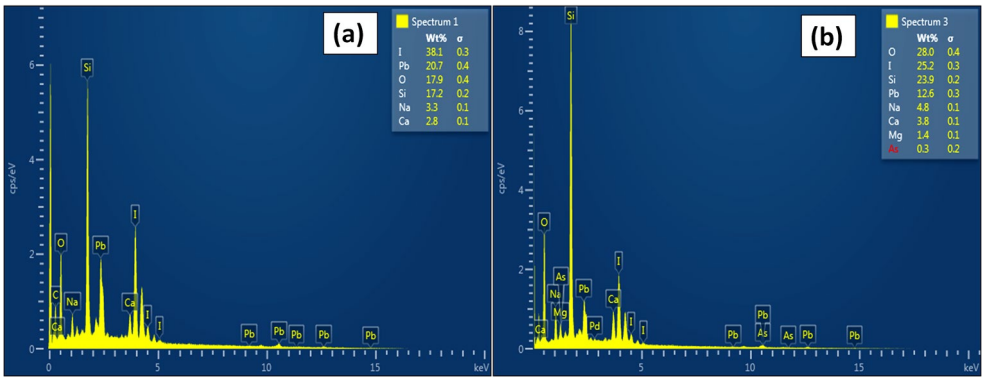

Fig. 4. EDS images of (a) Pristine Perovskite (b) Arsenic doped Perovskite

This technique leverages electron-excited characteristic X-ray peaks for the identification and quantification of elements across the periodic table, excluding Hydrogen (H), Helium (He), and

Lithium (Li) as they are predominant constituents. The elemental composition of $CH_3NH_3PbCl_3$ Perovskite, both un-doped and Arsenic-doped, has been determined through EDS measurements within the energy range of 1–20 keV. In this measurement we have taken 20keV for correct measurements. EDS mapping validated the presence of expected elements such as indium (In), lead (Pb), carbon (C), nitrogen (N), and iodine (I) without any impurities. In the spectra of doped perovskite, only constituent elements have been observed.

The atomic percentages (at %) of Ca, Na, Pb, and I in the synthesized perovskite powders are detailed in the accompanying table 1. Notably, the atomic proportion of lead to other elements [Pb/(Ca+Na+Pb+I)] exhibited an decrease with higher levels of doping of Arsenic, as outlined in the table. EDS measurements unequivocally confirmed the presence of Arsenic in the as-prepared perovskite samples. Basically, our EDS results demonstrated a systematic reduction in Pb content in Arsenic-doped perovskite, leading to a diminished toxicity level compared to their pristine (Pb-based) counterparts [25].

Table 1. Atomic percentages in pristine perovskite and as- doped perovskite.

Elements	Ca	Na	Pb	I	As
Pristine Perovskite	2.8	3.3	20.7	38.1	-
As-Doped Perovskite	4.8	4.8	12.6	25.2	0.3

The incorporation of arsenic in perovskite materials has been demonstrated to significantly enhance environmental safety. In essence, our research emphasizes the effectiveness of arsenic doping in perovskite materials, providing a promising direction for expanding their use and addressing environmental issues related to lead-based formulations.

In a planar device configuration, pristine and arsenic-doped perovskite solar cells were fabricated using a one-step method (Figure 1a and 1b). I-V curves of the devices (Figure 6b) and corresponding photovoltaic parameters (Table 2) were measured under optimized conditions. The photovoltaic performance of devices D1 was found to be significantly poorer compared to device D2, indicating the influence of arsenic doping (Table 2). The presence of several holes in the perovskite films of pristine perovskite (Figure 3a) led to serious charge recombination issues, partially mitigated by arsenic doping.

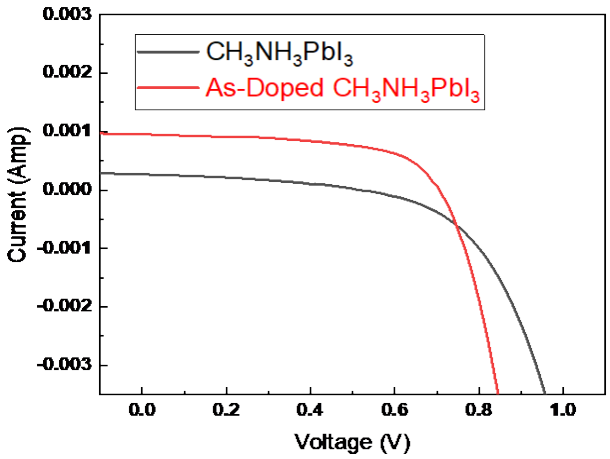

Fig. 5. I-V Graph of pristine Perovskite and Perovskite with doping of Arsenic

A full surface coverage was identified as crucial for high-performance perovskite solar cells. Introduction of a moderate amount of arsenic resulted in enhanced PCE due to improvements in Open Circuit Voltage (V_{oc}), Short-Circuit Current (I_{sc}), and Fill Factor (FF). The devices without arsenic exhibited a lower Shunt Resistance (R_{sh}) of 5185.68 ohms, which increased to 5724.31 ohms with the addition of arsenic in the precursor solution. This increase in R_{sh} suggests a reduction in defects, lowering the chance of charge recombination and contributing to the improved overall performance of the solar cells.

The increased in efficiency of devices based doped Arsenic can be explained by the balance of high R_{sh} and R_s. The efficiency spectra show a regular response (Figure 5). This can be attributed to the increased light absorption of the perovskite films, a smaller amount charge recombination and faster charge extraction [25–27].

Table 2. Photovoltaic parameters of Pristine Perovskites and As-Doped Perovskite.

Devices	V_{oc} (V)	I_{sc} (A)	(FF)	Efficiency (%)	Series Resistance (R_S)	Parallel Resistance (R_P)
Pristine Perovskite	0.51	0.00026	36.67	0.20	902.16	5185.68
As-Doped Perovskite	0.70	0.00094	58.23	1.55	94.75	5724.31

3. Conclusions

This study rigorously explores the influence of arsenic doping on the morphology, optical characteristics, and photovoltaic efficacy of perovskite films. The incorporation of arsenic leads to heightened light absorption, improved electron transport efficiency, and accelerated electron extraction from the perovskite layer to the electron transport layer. The fabrication process involves a straightforward one-step spin-coating method for both pristine perovskite solar cells and arsenic-doped counterparts, yielding champion Power Conversion Efficiencies (PCE) of 0.20% and 1.55%, respectively. Notably, this research not only introduces a simple and efficient approach for producing high-quality perovskite films but also highlights the reduced toxicity associated with arsenic-doped formulations, contributing to the overall advancement of perovskite solar cell technology.

References

[1] Kharkwal, D., Sharma, N., Gupta, S. K., Negi, C. M. S. (2021); Solar Energy, 230, 1133-1140; https://doi.org/10.1016/j.solener.2021.11.037

[2] Dada, M., Popoola, P. (2023), Beni-Suef University Journal of Basic and Applied Sciences, 12(1), 1-15; https://doi.org/10.1186/s43088-023-00405-5

[3] Singh, B. P., Goyal, S. K., Kumar, P. (2021), Materials Today: Proceedings, 43, 2843-2849; https://doi.org/10.1016/j.matpr.2021.01.003

[4] Sharma, N., Negi, C. M. S., Verma, A. S., Gupta, S. K. (2018), Journal of Electronic Materials, 47, 7023-7033; https://doi.org/10.1007/s11664-018-6629-3

[5] Goswami., R., Saha, R. (2022), Contemporary Trends in Semiconductor Devices. Springer Singapore; https://doi.org/10.1007/978-981-16-9124-9

[6] Sharma, N., Gupta, S. K., Negi, C. M. S. (2019), Superlattices and Microstructures, 135, 106278; https://doi.org/10.1016/j.spmi.2019.106278

[7] Yao, Z., Lum, Y., Johnston, A., Mejia-Mendoza, L. M., Zhou, X., Wen, Y., Seh, Z. W. (2023), Nature Reviews Materials, 8(3), 202-215; https://doi.org/10.1038/s41578-022-00490-5

[8] Sharma, N., Gupta, S. K., Negi, C. M. S. (2020), Journal of Materials Science: Materials in Electronics, 31, 22274-22283; https://doi.org/10.1007/s10854-020-04728-2

[9] Sharma, N., Negi, C. M. S., Sharma, M., Verma, A. S., Gupta, S. K. (2019), Optical Materials, 95, 109273; https://doi.org/10.1016/j.optmat.2019.109273

[10] Nayak, P. K., Mahesh, S., Snaith, H. J., Cahen, D. (2019), Nature Reviews Materials, 4(4), 269-285; https://doi.org/10.1038/s41578-019-0097-0

[11] Solak, E. K., & Irmak, E. (2023), RSC advances, 13(18), 12244-12269; https://doi.org/10.1039/D3RA01454A

[12] Khatibi, A., Razi Astaraei, F., Ahmadi, M. H. (2019), Energy Science & Engineering, 7(2), 305-322; https://doi.org/10.1002/ese3.292

[13] Chen, L. X. (2019), ACS Energy Letters, 4(10), 2537-2539; https://doi.org/10.1021/acsenergylett.9b02071

[14] Kojima, A., Teshima, K., Shirai, Y., Miyasaka, T. (2009), Journal of the american chemical society, 131(17), 6050-6051; https://doi.org/10.1021/ja809598r

[15] Lee, M. M., Teuscher, J., Miyasaka, T., Murakami, T. N., Snaith, H. J. (2012), Science, 338(6107), 643-647; https://doi.org/10.1126/science.1228604

[16] Chaudhary, S., Gupta, S. K., Negi, C. M. S. (2020), Materials Science in Semiconductor Processing, 109, 104916; https://doi.org/10.1016/j.mssp.2020.104916

[17] Phung, N., Félix, R., Meggiolaro, D., Al-Ashouri, A., Sousa e Silva, G., Hartmann, C., ... Abate, A. (2020), Journal of the American Chemical Society, 142(5), 2364-2374; https://doi.org/10.1021/jacs.9b11637

[18] Liu, Y., Huang, H., Xue, L., Sun, J., Wang, X., Xiong, P., Zhu, J. (2021), Nanoscale, 13(47), 19840-19856; https://doi.org/10.1039/D1NR05797A

[19] Tabassum, M., Zia, Q., Zhou, Y., Reece, M. J., Su, L. (2021), SN Applied Sciences, 3, 1-15; https://doi.org/10.1007/s42452-021-04877-x

[20] Li, X., Shi, J., Chen, J., Tan, Z., Lei, H. (2023), Materials, 16(12), 4490; https://doi.org/10.3390/ma16124490

[21] Eze, V. O., Carani, L. B., Majumder, H., Uddin, M. J., Okoli, O. I. (2022), Scientific Reports, 12(1), 7794; https://doi.org/10.1038/s41598-022-11729-0

[22] Zhang, L., Yuan, M. (2022), Light: Science & Applications, 11(1), 99; https://doi.org/10.1038/s41377-022-00782-z

[23] Aktas, E., Rajamanickam, N., Pascual, J., Hu, S., Aldamasy, M. H., Di Girolamo, D., Abate, A. (2022), Communications Materials, 3(1), 104; https://doi.org/10.1038/s43246-022-00327-2

[24] Zhao, Q., Li, G. R., Song, J., Zhao, Y., Qiang, Y., Gao, X. P. (2016), Scientific reports, 6(1), 38670; https://doi.org/10.1038/srep38670

[25] Suzuki, A., Okada, H., Oku, T. (2016), Energies, 9(5), 376; https://doi.org/10.3390/en9050376

[26] Hasanzadeh Azar, M., Aynehband, S., Abdollahi, H., Alimohammadi, H., Rajabi, N., Angizi, S., Simchi, A. (2023, March), Photonics (Vol. 10, No. 3, p. 271). MDPI; https://doi.org/10.3390/photonics10030271

[27] Khan, M. I., Mukhtar, A., Alwadai, N., Irfan, M., Haq, I. U., Albalawi, H., Iqbal, M. (2022), Coatings, 12(3), 386; https://doi.org/10.3390/coatings12030386